Restoration of Euglycemia After Duodenal Bypass Surgery Is Reliant on Central and Peripheral Inputs in Zucker *fa/fa* Rats

Jian Jiao,[1] Eun Ju Bae,[2] Gautam Bandyopadhyay,[2] Jason Oliver,[1] Chaitra Marathe,[1] Michael Chen,[1] Jer-Yuan Hsu,[1] Yu Chen,[1] Hui Tian,[1] Jerrold M. Olefsky,[2] and Maziyar Saberi[1]

Gastrointestinal bypass surgeries that result in rerouting and subsequent exclusion of nutrients from the duodenum appear to rapidly alleviate hyperglycemia and hyperinsulinemia independent of weight loss. While the mechanism(s) responsible for normalization of glucose homeostasis remains to be fully elucidated, this rapid normalization coupled with the well-known effects of vagal inputs into glucose homeostasis suggests a neurohormonally mediated mechanism. Our results show that duodenal bypass surgery on obese, insulin-resistant Zucker *fa/fa* rats restored insulin sensitivity in both liver and peripheral tissues independent of body weight. Restoration of normoglycemia was attributable to an enhancement in key insulin-signaling molecules, including insulin receptor substrate-2, and substrate metabolism through a multifaceted mechanism involving activation of AMP-activated protein kinase and downregulation of key regulatory genes involved in both lipid and glucose metabolism. Importantly, while central nervous system–derived vagal nerves were not essential for restoration of insulin sensitivity, rapid normalization in hepatic gluconeogenic capacity and basal hepatic glucose production required intact vagal innervation. Lastly, duodenal bypass surgery selectively altered the tissue concentration of intestinally derived glucoregulatory hormone peptides in a segment-specific manner. The present data highlight and support the significance of vagal inputs and intestinal hormone peptides toward normalization of glucose and lipid homeostasis after duodenal bypass surgery. ***Diabetes*** **62:1074–1083, 2013**

Obesity is commonly associated with insulin resistance and type 2 diabetes (1). The most effective therapy for alleviating obesity is bariatric surgery (2). In addition to its long-term impact on body weight, a rapid restoration of euglycemia is observed in diabetic patients preceding substantial weight loss (3,4). Despite widespread appreciation of this phenomenon, little is known regarding the underlying mechanism(s). Because insulin resistance is usually a prerequisite for the development of type 2 diabetes, bariatric surgery likely improves insulin sensitivity. To this end, alterations in hormonal milieu and glucomodulatory effects mediated by the gut-brain axis represent two plausible mechanisms. For evaluation of these mechanisms, glucose clamp studies were undertaken in Zucker *fa/fa* (ZF) rats after duodenal-jejunal bypass surgery (DJB) with and without total subdiaphragmatic vagotomy (TSV). Furthermore, to determine whether improvement in glucoregulation is in part mediated by changes in intestinally derived hormone peptides, we assessed circulating and tissue concentration of a select set of intestinal factors. Our data indicate that DJB was sufficient to rapidly restore euglycemia in ZF rats. This normalization was attributable to improved lipid metabolism, altered patterning of intestinally derived hormones, and insulin sensitivity but was independent of body weight, food intake, and augmented insulin secretion. Importantly, denervation studies underscored the importance of central nervous system (CNS)-derived vagal inputs with respect to hepatic gluconeogenic capacity and regulation of hepatic glucose production (HGP) after DJB.

RESEARCH DESIGN AND METHODS

Selection of animal model. Goto-Kakizaki (GK), diet-induced obesity Sprague-Dawley and Wistar rats, and the obese, insulin-resistant ZF rats have previously been used to examine the impact of bariatric surgery on glucose homeostasis (5–8). Our data (Supplementary Fig. 1*A* and *B*) indicate that while both Sprague-Dawley and Wistar rats become obese and develop fatty liver after 30 weeks of high-fat diet, rats remain euglycemic with no apparent defect in glycemic control. While the reasons for lack of diet-induced insulin resistance are unclear, it is plausible that compensatory glucose disposal by peripheral tissues or increased glucose excretion provides a protective mechanism. As such, it is difficult to evaluate modalities that modulate insulin sensitivity in these animal models. The GK rat has stable hyperglycemia; however, the lack of obesity and peripheral insulin resistance limits its use for elucidating mechanisms of obesity-induced insulin resistance. Considering these limitations, we elected to characterize the impact of DJB in the obese, hyperlipidemic, hyperinsulinemic, insulin-resistant ZF rat.

Surgical procedures and in vivo metabolic assessments. All surgical procedures were performed on 11- to 13-week-old male ZF rats and metabolic studies 1 month post-surgery. DJBs were carried out as previously described (9). Sham-operated animals were exposed to similar surgical conditions and pair-fed when appropriate. Oral glucose tolerance tests (oGTTs) (1 g/kg) and mixed-meal tolerance tests (mmTTs) (15 g normal rat chow) were carried out after an overnight fast. For intravenous glucose tolerance test (ivGTTs) (1 g/kg), animals were cannulated in the jugular vein and glucose was injected in bolus. For assessment of hepatic gluconeogenic capacity, intraperitoneal pyruvate tolerance test (ipPTT) (1 g/kg) was conducted in overnight-fasted animals. For assessment of tissue-specific insulin sensitivity, hyperinsulinemic-euglycemic clamp procedures were conducted as previously described with minor modifications (10). Briefly, after an overnight fast, at −130 min a priming dose of 7.5 μCi D-[3-^{3}H]glucose (PerkinElmer) was administered into the carotid artery and a constant-rate (0.167 μCi/min; 16.7 μL/min) infusion of D-[3-^{3}H]glucose was started at –120 min. Blood samples (25 μL in duplicate) were taken at −30, −20, −10, and 0 min for measurement of tracer-specific activity for assessment of basal HGP. At time 0 min (i.e., after 120 min of tracer equilibration), glucose (variable infusion, 50% dextrose; Hospira) and tracer plus insulin (25 mU/kg/min; Humulin, Eli Lilly) infusions were started simultaneously. Steady-state glucose concentrations were maintained for at

From [1]NGM Biopharmaceuticals, Inc., South San Francisco, California; and the [2]Department of Medicine, University of California, San Diego, La Jolla, California.

Corresponding authors: Jerrold M. Olefsky, jolefsky@ucsd.edu, and Maziyar Saberi, msaberi@ngmbio.com.

Received 25 May 2012 and accepted 8 October 2012.

DOI: 10.2337/db12-0681

This article contains Supplementary Data online at http://diabetes.diabetesjournals.org/lookup/suppl/doi:10.2337/db12-0681/-/DC1.

See accompanying commentary, p. 1012.

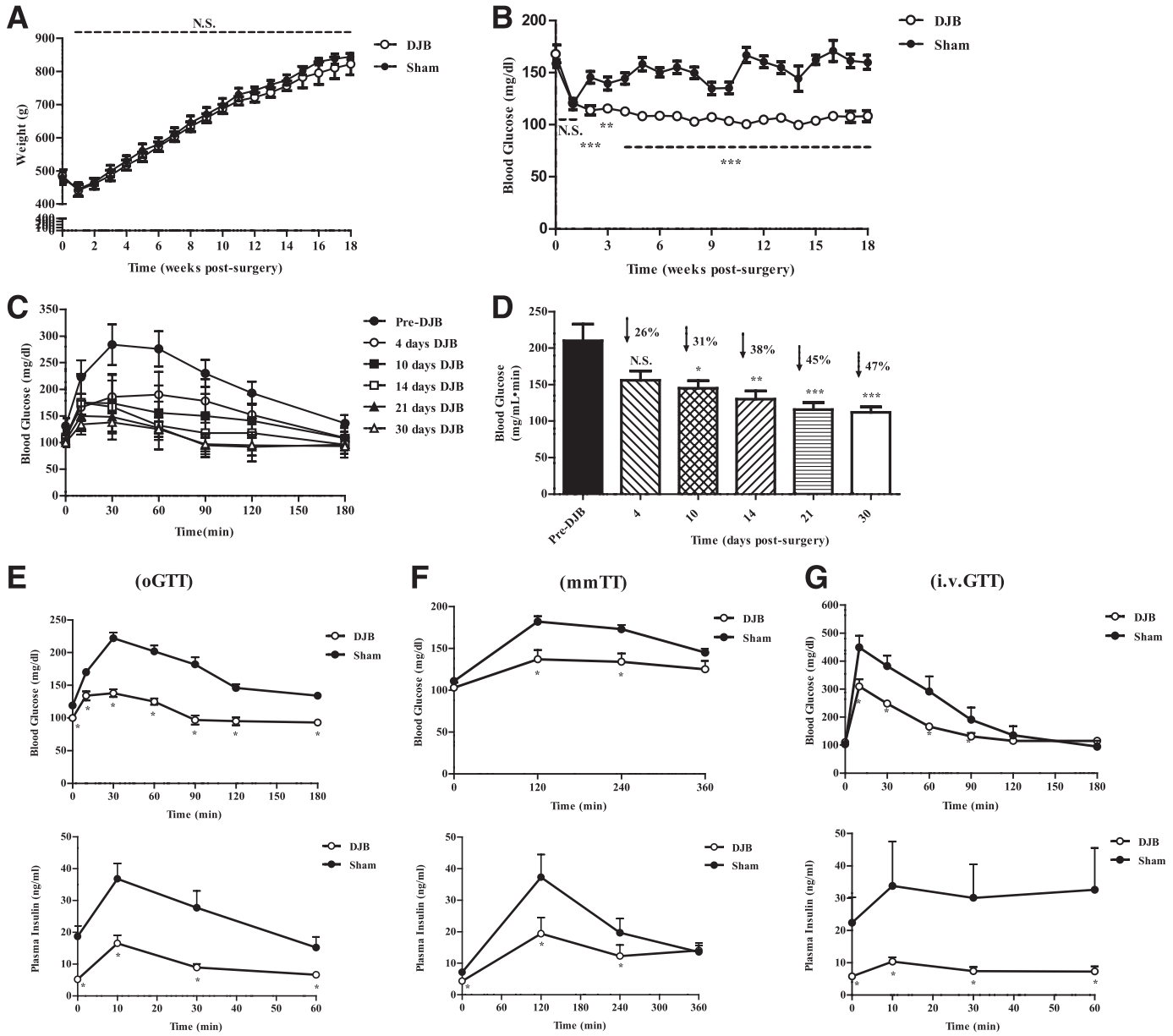

FIG. 1. DJB ameliorates glucose intolerance independent of body weight and augmented insulin secretion. *A*: DJB did not alter body weight compared with sham-operated, pair-fed, age-matched animals (sham). All surgeries were conducted between 9 and 11 weeks of age. *B*: DJB significantly reduced postprandial blood glucose concentration compared with sham. *C*: Time-course evaluation of oGTT beginning day four postsurgery. DJB rapidly improved oral glucose tolerance, reaching a plateau prior to day 30. *D*: Area under the curve (AUC) calculation for time-course oGTT studies from *C*. DJB continuously improved oGTT, reaching a plateau by day 30 post-surgery. *E*: DJB improved glucose tolerance, fasted insulin concentration, and glucose-stimulated insulin secretion compared with sham. *F*: DJB improved mmTT and mixed-meal–stimulated insulin secretion compared with sham. *G*: DJB improved intravenous glucose tolerance and glucose-stimulated insulin secretion compared with sham. All experiments consisted of $n \geq 6$/group. All studies were conducted in age-matched animals with no significant difference in body weight. Separate sets of animals were used for each metabolic study. *$P < 0.05$, **$P < 0.01$, ***$P < 0.001$. N.S., not significant. Values are means ± SEM.

least 40 min for assessment of tracer-specific activity. For assessment of β-cell function, hyperglycemic clamps were conducted as previously described (11). All rats were individually housed on a 12:12-h light:dark cycle. Animals were fed a standard rodent chow (2018; Tekland Global) and water ad libitum. All animal care procedures and experimental procedures were approved by the institutional animal care and use committee at NGM Biopharmaceuticals, Inc. All animals were obtained from Harlan Laboratories.

Indirect calorimetry. Studies were conducted using the TSE PhenoMaster Systems 1 month post-DJB. Animals were acclimated to the metabolic cages for a period of 36 h prior to a 72-h study period.

TSV. TSV was performed 1 month post-DJB. The timing for TSV was selected to confirm the positive effect of DJB on glucose tolerance prior to examining the contribution of vagal nerves. The surgical procedures for TSV have previously been described in detail (12). Control animals underwent identical surgical procedures including isolation of the hepatic and subdiaphragmatic trunks, but the nerves were left intact.

Tissue collection and analysis. Quadriceps, liver, and visceral fat tissues were harvested for measuring the mRNA and protein content of insulin-signaling molecules 1 month after surgery. For insulin-stimulated assays, animals were intraportally infused with Humulin at 0.5 units/kg for 6 min and tissues were excised in a timely manner and later homogenized in Tris lysis buffer (50 mmol/L Tris, pH 8.0; 150 mmol/L NaCl; 1% Triton X-100; and 0.1% SDS) containing protease inhibitor and phosphatase inhibitor cocktails (Sigma). Protein concentration was measured and adjusted to the same concentration across the samples. Samples were diluted with assay buffer provided by Bio-Rad. Triacylglyceride (TAG) and diacylglyceride (DAG) measurements were carried out as previously described (13). Ceramide content was analyzed using recombinant ceramide kinase (BPS Biosciences, San Diego, CA; catalog number

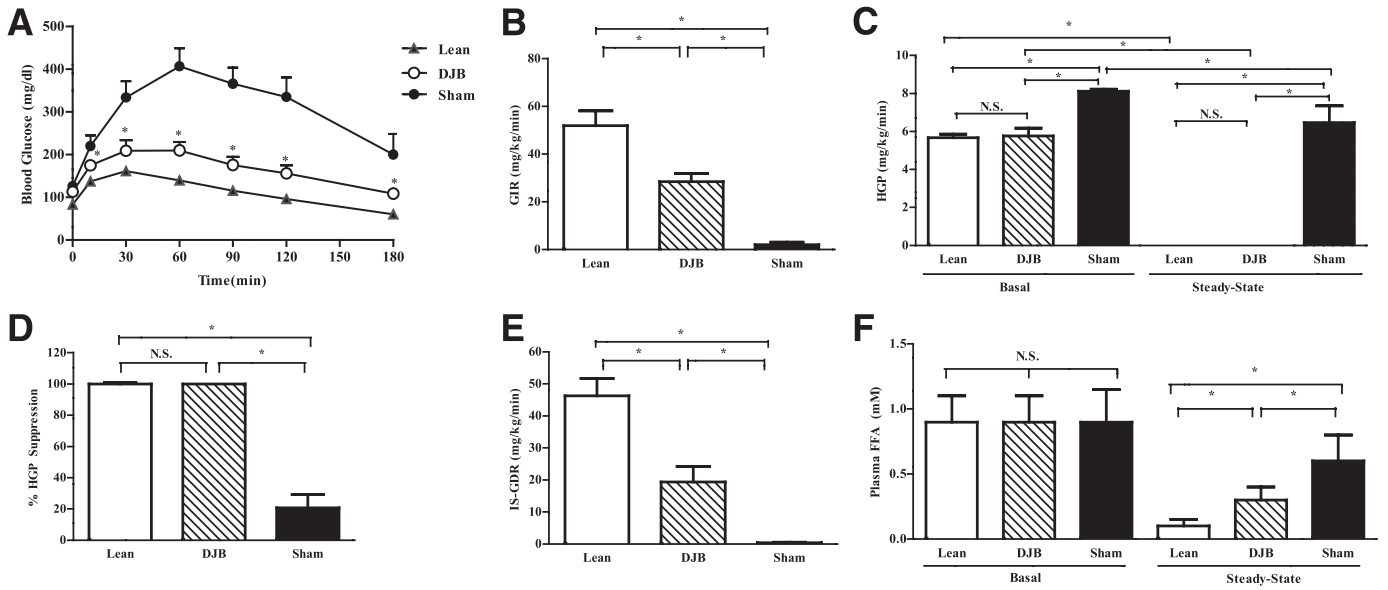

FIG. 2. DJB improves gluconeogenic capacity and hepatic and peripheral insulin sensitivity. *A*: DJB improved hepatic gluconeogenic capacity as assessed by PTT. *B*: GIR, a measure of systemic insulin sensitivity, was increased in DJB compared with sham during hyperinsulinemic-euglycemic clamps but remained lower compared with lean. *C*: HGP before (basal) and during (insulin stimulated) the steady state improved in DJB compared with sham during hyperinsulinemic-euglycemic clamps. Basal HGP and hepatic insulin sensitivity were fully restored in DJB compared with lean during hyperinsulinemic-euglycemic clamps. *D*: Insulin-mediated suppression of HGP, an assessment of hepatic insulin sensitivity, is fully restored in DJB compared with lean during hyperinsulinemic-euglycemic clamps. *E*: Skeletal muscle insulin sensitivity (IS-GDR) is improved in DJB but remains impaired compared with lean during hyperinsulinemic-euglycemic clamps. *F*: Insulin-mediated (steady-state) suppression of adipose tissue–derived free fatty acids (FFAs) (lipolysis) is improved in DJB but remained impaired compared with lean during hyperinsulinemic-euglycemic clamps. All experiments were conducted 1 month post-DJB surgery in age-matched animals. Body weight was not different between DJB and sham, but both were significantly heavier compared with lean. All experiments consisted of $n \geq 8$/group. *$P < 0.05$. N.S., not significant. Values are means ± SEM.

40617) following the same kinase assay protocol used by the manufacturer. All reagents required to assay lipid contents were purchased from WAKO (Richmond, VA). Protein content was assayed in an aliquot by bicinchoninic acid method. Fatty acid oxidation was determined using previously established procedures (14). Glycogen was assayed as previously described (15). Western blots were performed using 4–12% SDS-PAGE acrylamide gels (Invitrogen, CA). Antibodies were purchased from Cell Signaling Technology (Danvers, MA). Total RNA was isolated using TRIzol (Invitrogen). First-strand cDNA was synthesized using a high-capacity cDNA reverse-transcription kit (Applied Biosystems, Foster City, CA). The samples were run in 20-μl reactions using an MJ Research PTC-200 96-well thermocycler coupled with the Chromo4 four-color real-time system (GMI, Ramsey, MN). Gene expression levels were calculated as previously described (16). Primer information is available in Supplementary Table 2.

Intestinal hormone peptide extraction and analysis. DJB, sham-operated and their Zucker lean littermates were fasted overnight followed by a 2-h refeeding with 15 g normal chow. Intestines were collected and divided into duodenum, jejunum, ileum, and colon segments. The intestinal segments were cut open longitudinally, rinsed with PBS twice, and immediately frozen in liquid nitrogen. The segments were then weighed and immersed in extraction buffer (methanol with 0.1% trifluoroacetic acid), 5 mL buffer/g tissue, in 50-mL conical tubes rotating for 1 h at room temperature. The tissues were centrifuged at 3,500 rpm for 10 min, and the supernatants were filtered, vacuum dried, and reconstituted in PBS. Total protein concentration was measured using BCA Protein Assay Reagent (Thermo Scientific). The peptides were measured using ELISA kits: glucagon-like peptide-1 (GLP-1), (active 7-36; Alpco and Millipore), glucose-dependent insulinotropic peptide (GIP) (rat/mouse total; Millipore), and peptide YY (PYY) (mouse/rat; Alpco).

Statistics and calculations. Experimental results are expressed as means ± SEM. Results were tested statistically by an unpaired two-tailed Student t test or one-way ANOVA with the Bonferroni correction using GraphPad Prism 5.0 (San Diego, CA). The criterion for statistical significance was set at $P < 0.05$.

RESULTS

Nonrestrictive proximal intestinal bypass surgery ameliorates obesity-induced glucose intolerance and hyperinsulinemia independent of weight loss. To determine whether reduction in body weight was a prerequisite for restoration of euglycemia, we performed DJB, a nonrestrictive surgery. DJB resolved hyperglycemia compared with sham-operated, pair-fed animals (sham) independent of body weight (Fig. 1*A* and *B*). The ideal time for detailed metabolic studies, defined by full recovery from surgery and metabolic stability, was determined based on data gathered from time course oGTT studies (Fig. 1*C* and *D*). DJB rapidly improved glucose tolerance, reaching a plateau prior to week 4. Therefore, we elected to examine the impact of DJB on insulin sensitivity at this time point. To assess nutrient-induced insulin secretion, we conducted oGTT and mmTT in separate sets of animals (Fig. 1*E* and *F*). Peak glucose and insulin excursion was reduced by ~40 and ~55%, respectively, indicating that whole-body glucose disposal was increased independent of augmented insulin secretion. To account for potential metabolic responses attributable to delayed gastric emptying or malabsorption, ivGTT was performed (Fig. 1*G*). Similarly, glucose and insulin excursion was reduced by ~30 and ~75%, respectively. When the peak insulin concentration of DJB during oGTT and mmTT was compared with that from ivGTT, a modest incretin effect was observed; however, it remained significantly lower compared with respective controls.

Duodenal bypass surgery restores HGP and ameliorates hepatic and peripheral insulin sensitivity. Increased hepatic glucose output is an important cause of fasting hyperglycemia (17). Elevated HGP is attributed to increased gluconeogenesis (18). To assess hepatic gluconeogenic capacity, we performed ipPTT and found that the glucose excursion in DJB was reduced by ~50% compared with sham (Fig. 2*A*). For accurate assessment and dissociation of basal HGP from hepatic and peripheral insulin sensitivity, hyperinsulinemic-euglycemic clamp studies were

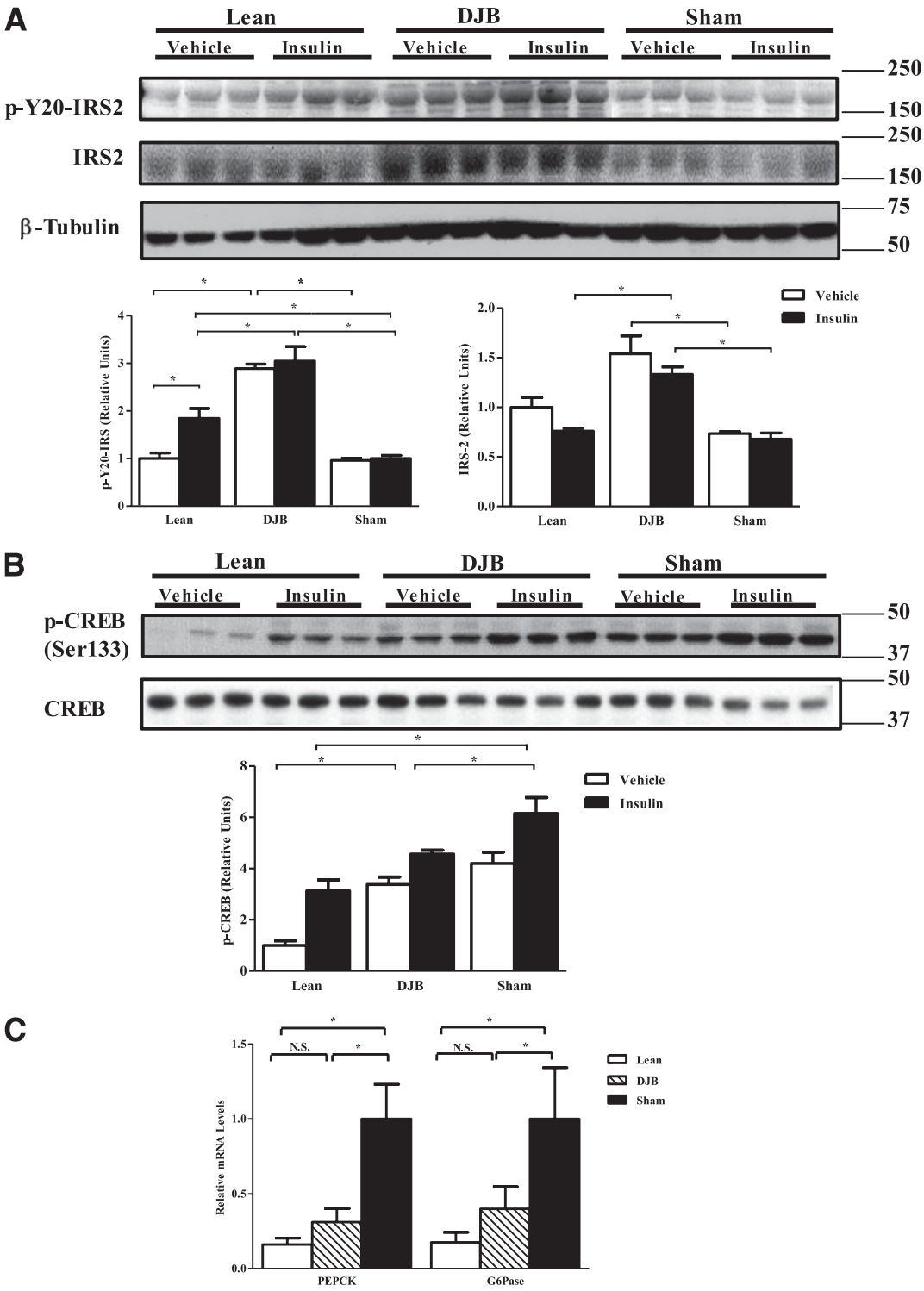

FIG. 3. Proximal intestine bypass surgery improves hepatic insulin signaling and expression of key gluconeogenic enzymes. *A*: Total and tyrosine phosphorylation (p-Y20) of IRS-2. DJB significantly increases total, basal (vehicle), and insulin-stimulated (insulin) p-Y20 compared with both sham and lean. *B*: Consistent with improved HGP, DJB decreased phosphorylation of CREB. *C*: Consistent with improved gluconeogenic capacity and improved HGP, DJB normalized expression of key genes involved in hepatic gluconeogenesis: *PEPCK* and *G6Pase*. All experiments were conducted 1 month post-surgery. A separate set of animals was used for basal (vehicle) and insulin-stimulated (insulin) tissue analysis. All experiments consisted of $n \geq 8$/group. *$P < 0.05$. N.S., not significant. Values are means ± SEM.

performed. Body weights were similar between DJB and sham, and both groups were markedly obese compared with the lean group (Supplementary Fig. 1*C*). However, postprandial and fasted insulin concentrations were approximately twofold lower in DJB compared with sham (Supplementary Fig. 1*D*). The exogenous glucose infusion rate (GIR) required to maintain euglycemia (~100 mg/dL) was markedly higher in DJB compared with sham, confirming enhanced systemic insulin sensitivity (Fig. 2*B*). The improvement in GIR was due to restoration of basal HGP;

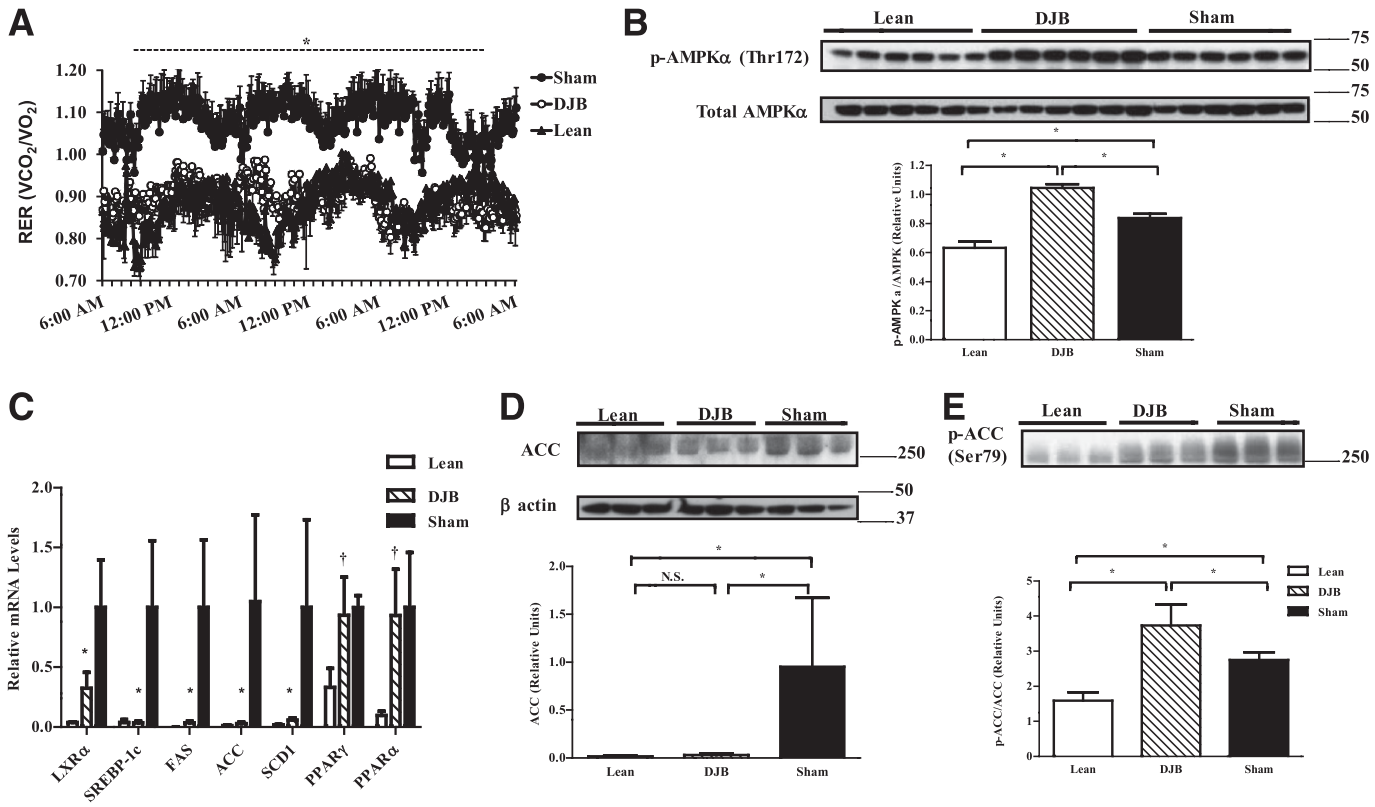

FIG. 4. DJB enhances lipid oxidation and reduces lipogenesis. *A*: RER, a measure of fuel-type use, is normalized in DJB compared with lean. Decreased RER values in DJB suggest a shift toward enhanced lipid use. *B*: Consistent with enhanced lipid utilization, DJB increased phosphorylation of AMPK compared with sham and lean. *C*: Expression of key genes involved in lipogenesis and lipid oxidation are either dramatically improved or normalized compared with lean (*D*). Total protein content of ACC is normalized in DJB compared with lean. *E*: Consistent with enhanced lipid metabolism, DJB increases phosphorylation of ACC compared with sham and lean. All experiments were conducted 1 month postsurgery. All experiments consisted of $n \geq 8$/group. For panel *C*: †Significantly different from Lean, $P < 0.05$. *Significantly different from lean and sham, $P < 0.05$. For panels *A*, *B*, *D*, and *E*: *$P < 0.05$. N.S., not significant. Values are mean ± SEM.

hepatic insulin sensitivity, as indicated by enhanced insulin-mediated suppression of HGP; and an increase in insulin-stimulated glucose disposal rate (IS-GDR), a marker for skeletal muscle insulin sensitivity (Fig. 2*C*–*E*). Insulin-mediated suppression of adipose tissue–derived free fatty acids was also greater in DJB, signifying increased adipocyte insulin sensitivity (Fig. 2*F*). Intriguingly, steady-state plasma insulin concentration was lower in DJB compared with sham (Supplementary Fig. 1*E*). This reduction was attributed to an increased metabolic clearance rate of insulin (Supplementary Fig. 1*F*).

For determination of whether DJB altered insulin secretion, hyperglycemic clamp studies were conducted (Supplementary Fig. 1*G*). Glucose-stimulated insulin secretion was lower in DJB during physiologically relevant bouts of hyperglycemia (Supplementary Fig. 1*H*). However, insulin concentration was not statistically different between DJB and sham at supraphysiological glucose levels (i.e., >350 mg/dL), suggesting that the maximal secretory capacity was not compromised. Insulin sensitivity after DJB was further confirmed, as GIR was increased by ~80% (Supplementary Fig. 1*I*).

To understand the mechanism of improved insulin sensitivity, we measured key aspects of the insulin-signaling pathway. We observed an increase in total content and tyrosine phosphorylation of insulin receptor substrate (IRS)-2 in DJB liver in both the basal and insulin-stimulated states (Fig. 3*A*). Surprisingly, insulin-stimulated Akt phosphorylation was not different among the groups (Supplementary Fig. 2*A*). Phosphorylation of cAMP response element–binding protein (CREB), a key regulator of hepatic gluconeogenesis (19), was reduced in DJB liver (Fig. 3*B*) without any changes in hepatic glycogen content (Supplementary Fig. 2*B*). The expression of the key gluconeogenic genes phosphoenolpyruvate carboxykinase (*PEPCK*) and glucose 6-phosphatase (*G6Pase*) was also decreased (Fig. 3*C*).

Improved insulin sensitivity is concomitant with enhanced β-oxidation and reduced lipogenesis. To ascertain whether enhanced systematic insulin sensitivity was attributable to enhanced lipid oxidation, we performed indirect calorimetry (Supplementary Table 1). Although body weight, food intake, and water consumption and activity levels were not different between groups, we observed a small increase in body temperature. Remarkably, lipid use was increased in DJB and normalized to lean, as indicated by a lower respiratory exchange ratio (RER) (Fig. 4*A*). To evaluate whether DJB rats remained metabolically flexible, we performed similar tests in separate sets of animals exposed to an overnight fast. DJB and sham responded similarly when fasted, relying exclusively on lipid oxidation, but returned to prefasting conditions when reexposed to food (Supplementary Fig. 3*A*). Consistent with the RER values, plasma TAG was reduced without a change in TAG secretion capacity in DJB, while fasted total ketones and β-hydroxybutyrate, indirect markers of lipid oxidation, were increased by ~40 and ~50% in DJB compared with sham, respectively (Supplementary Fig. 3*B*–*E*).

TABLE 1
DJB improves lipid metabolism in liver, skeletal muscle, and adipose tissue

	Lean	DJB	Sham
Liver			
FA-CoA (μmol/g)	1.47 ± 0.22†	0.42 ± 0.05*†	0.80 ± 0.1*
DAG (μmol/g)	3.10 ± 0.34†	6.80 ± 0.74*†	9.20 ± 0.81*
Ceramide (μmol/g)	0.84 ± 0.11†	1.02 ± 0.06†	1.66 ± 0.24*
TAG (μmol/g)	7.50 ± 0.85†	29.50 ± 3.3*	26.3 ± 2.7*
Palmitate oxidation (cpm/μmol/mg protein)	3,589 ± 300†	4,547 ± 150*†	2,419 ± 100*
Skeletal muscle			
FA-CoA (μmol/g)	0.88 ± 0.07†	0.23 ± 0.03*†	0.44 ± 0.05*
DAG (μmol/g)	0.78 ± 0.12†	0.94 ± 0.12†	1.60 ± 0.22*
Ceramide (μmol/g)	1.03 ± 0.08	0.47 ± 0.06*†	1.33 ± 0.12
TAG (μmol/g)	5.20 ± 0.82†	7.30 ± 0.85*†	11.50 ± 1.82*
Palmitate oxidation (cpm/μmol/mg protein)	1,340 ± 53†	1,193 ± 162†	684 ± 110*
Visceral fat			
FA-CoA (μmol/g)	5.24 ± 0.87	2.55 ± 0.33*†	4.15 ± 0.62
DAG (μmol/g)	69 ± 9.2†	52.4 ± 6.2†	83 ± 4.4
Ceramide (μmol/g)	3.12 ± 0.52†	2.74 ± 0.32†	5.05 ± 0.73*
TAG (μmol/g)	491.4 ± 17	476 ± 56	532.3 ± 73

Data are means ± SEM. All experiments consisted of $n \geq 8$/group. †Significantly different from sham animals, $P < 0.05$. *Significantly different from lean, $P < 0.05$.

To more accurately assess lipid use in liver, we measured hepatic palmitate oxidation. Palmitate oxidation was increased by ~90% in DJB liver compared with sham (Table 1). This increase was paralleled by phosphorylation of AMP-activated protein kinase (AMPK) (Fig. 4*B*). The expression of key regulatory genes in lipid metabolism was also examined (Fig. 4*C*). Expression of liver-X receptor α (*LXRα*), a key regulator of genes involved in lipid metabolism, was dramatically reduced. Expression of sterol regulatory element-binding protein-1c (*SREBP-1c*) along with its transcription targets, fatty acid synthase (*FAS*) and stearoyl-CoA desaturase 1 (*SCD-1*), was reduced, while expression of peroxisome proliferator–activated receptor (PPAR) γ and α remained unchanged. The expression of acetyl-CoA carboxylase (*ACC*), a rate-limiting enzyme in fatty acid synthesis, was decreased and its phosphorylation increased after DJB (Figs. 4*D* and *E*). Collectively, these findings provide a mechanism for the reduction of hepatic lipid synthesis and enhanced lipid oxidation associated with DJB.

We also measured specific hepatic lipid levels and observed a reduction in DAG, ceramides, and fatty acyl-CoAs (FA-CoAs), while hepatic TAG content was not altered (Table 1). Consistently, histological examination of lipid content did not reveal a difference between DJB and sham (Supplementary Fig. 3*F*).

To further characterize the impact of DJB on insulin-sensitive peripheral tissues, we measured markers of lipid metabolism and insulin signaling in muscle and visceral fat. Similar to liver, skeletal muscle palmitate oxidation was enhanced and was associated with activation of AMPK (Table 1 and Supplementary Fig. 4*A*). Unlike the liver, skeletal muscle Akt phosphorylation was increased and was paralleled by a reduction in glycogen stores (Supplementary Fig. 4*B* and *C*). Moreover, skeletal muscle concentrations of TAG, FA-CoA, DAG, and ceramides were equally reduced in DJB (Table 1). In visceral fat, DAGs, FA-CoAs, and ceramides were equally reduced without a change in TAG content (Table 1). This improvement was associated with an increase in insulin-stimulated Akt phosphorylation (Supplementary Fig. 4*D*).

DJB surgery increases intestinal mass and concentrations of select hormone peptides in a segment-specific manner. Gastrointestinal bypass surgery is accompanied by an array of physical and neurohormonal changes within the gastrointestinal system. While the circulating concentration of several intestinally derived factors, including GLP-1, GIP, and PYY, have previously been documented, it is not clear whether local tissue concentration of these peptides is equally altered. Therefore, we developed a method to extract peptides from the intestines in a segment-specific manner and evaluated the tissue content of GLP-1, GIP, and PYY. The duodenal and ileal mass was selectively increased in DJB (Fig. 5*A*). Although the plasma concentration of GIP and PYY was not altered after DJB (data not shown), their tissue concentration was dramatically increased in jejunum and ileum, respectively (Fig. 5*B* and *C*). Conversely, while tissue concentrations of GLP-1 were unaltered in DJB, GLP-1 concentration was increased in plasma postprandially and in response to refeeding (Fig. 5*D* and *E*). The divergence between the serum and tissue concentration of these peptides suggests that intestinally derived hormones, in addition to their endocrine mode of action, might exert effects through an autocrine and/or paracrine manner, perhaps by modulating the enteric nervous system. In support of this, both GLP-1 and PYY receptors are expressed on these glucomodulatory nerves innervating the gastrointestinal track (20–22).

Vagal innervation is required for regulation of gluconeogenic capacity and basal HGP but not hepatic and peripheral insulin sensitivity. On the basis of well-established effects of vagal inputs into glucose homeostasis (23), we examined the potential contribution of vagal signaling to the enhanced glucose metabolism after DJB. To account for potential contribution of all subbranches of the vagus nerve, we performed TSV in control ZF rats (TSV) (Supplementary Fig. 5*A*) and DJB-operated rats (DJB^{TSV}). Control animals were exposed to both sham DJB and TSV surgeries and were pair-fed to TSV animals (sham). At the time of metabolic studies, body weight was not different among groups (Supplementary Fig. 5*B*). Denervation was confirmed during surgery by monitoring of the heart rate response and postmortem by visual inspection of severed nerves (Supplementary Fig. 5*C*–*E*). For assessment of the immediate effect of vagotomy in DJB^{TSV}, ipPTT was performed 1 week post-surgery. While vagotomy did not further exacerbate glucose production in control ZF rats, TSV abolished DJB-induced normalization of gluconeogenic capacity (Fig. 6*A*). For determination of whether CNS-derived vagal nerves are required for maintenance of hepatic and peripheral insulin sensitivity, euglycemic-hyperinsulinemic clamps were performed. Consistent with the glucoregulatory role of vagal innervation, TSV abolished DJB-induced improvement in basal HGP (Fig. 6*B*). However, GIR during clamp studies remained markedly higher in DJB^{TSV} animals, indicating that DJB-induced improvement in insulin sensitivity was preserved independent of vagal innervation (Fig. 6*C*). In accord with the higher

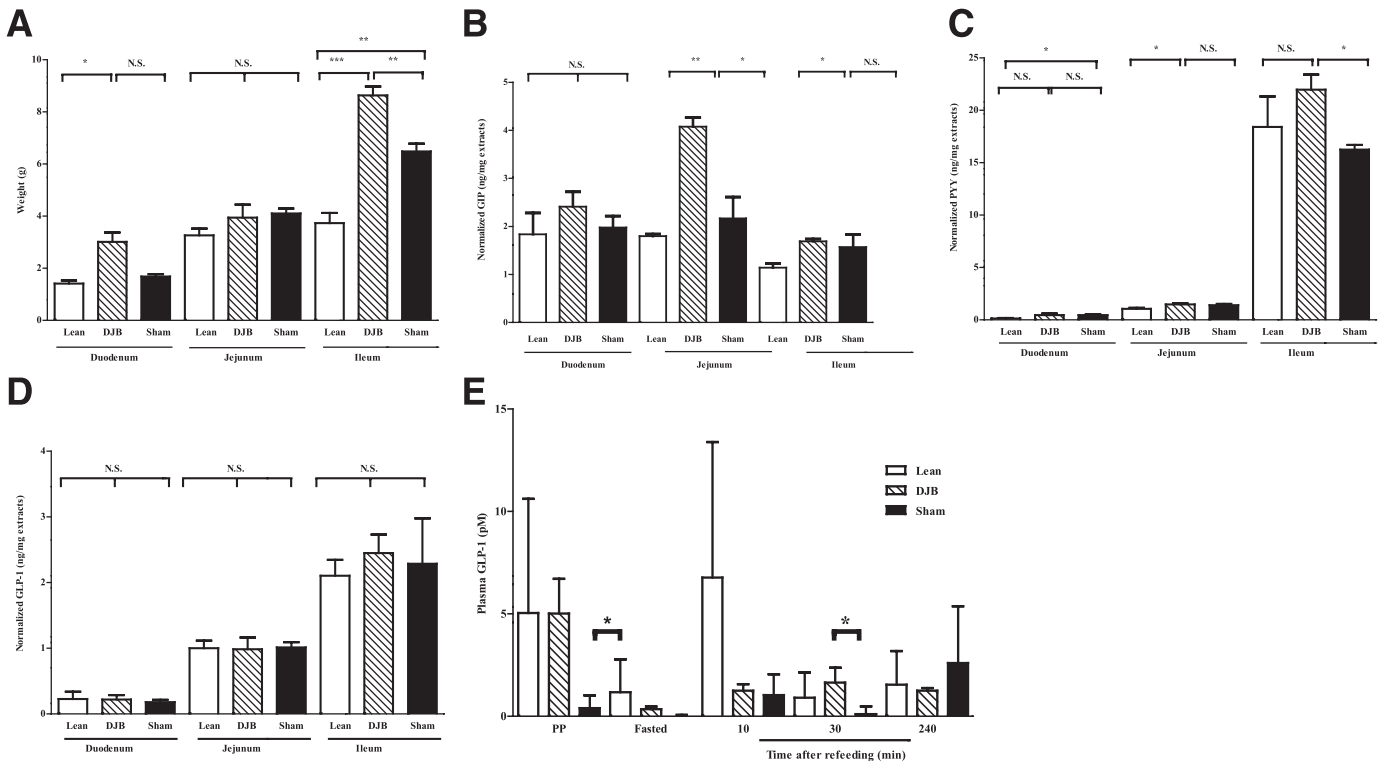

FIG. 5. DJB increases intestinal mass and concentration of select hormone peptides in a segment-specific manner. *A*: DJB selectively increases ileal mass compared with sham and lean. *B*: Concentration of GIP is increased in jejunum of DJB compared with sham and lean. *C*: Concentration of PYY is selectively normalized in ileum of DJB compared with lean. *D*: Intestinal concentration of GLP-1 is not altered by DJB. *E*: DJB normalizes circulating concentration of GLP-1 postprandially and in response to a standard mmTT compared with lean. All experiments consisted of $n \geq 6$/group. *$P < 0.05$. **$P < 0.01$. ***$P < 0.001$. N.S., not significant. Values are means ± SEM.

GIR, insulin-stimulated (steady-state) suppression of HGP, a marker of hepatic insulin sensitivity, and IS-GDR, a marker for skeletal muscle insulin sensitivity, remained markedly improved in the DJB^{TSV} (Fig. 6*D–F*). Adipocyte insulin sensitivity was also maintained in DJB^{TSV} (Fig. 6*G*). In fact, restoration of hepatic and peripheral insulin sensitivity was the same in DJB compared with DJB^{TSV} (compare Figs. 2 and 6), demonstrating that vagotomy failed to compromise the insulin-sensitizing effects of DJB.

DISCUSSION

Bariatric surgery is an increasingly popular and effective means to achieve substantial weight loss in obese patients, resulting in a wide range of improved health outcomes (24). In many post-surgical diabetic patients, antidiabetes medications can be stopped altogether, and oftentimes the underlying diabetic state is normalized within days and sustained for years. Of interest, nonrestrictive surgeries that simply bypass the duodenum similarly improve glucose homeostasis in the absence of weight loss. Collectively, these findings have generated great interest in understanding the mechanisms regulating metabolic balance after duodenal bypass.

The mechanisms underlying the metabolic effects of bariatric surgery are largely unknown, but several possibilities exist. *1*) Decreased caloric intake can have an immediate beneficial effect on glucose homeostasis. *2*) Gastrointestinal-CNS communication via the vagus nerve may contribute to enhanced glucose tolerance, HGP, and insulin sensitivity (25–28). *3*) Duodenal bypass could lead to the amplification as well as generation of novel gut hormone peptides(s) that improve insulin sensitivity or, alternatively, could suppress the secretion of a gut-derived diabetogenic factor(s). *4*) Finally, changes in bile acids and alteration in the intestinal microflora can favorably modulate obesity and glucose homeostasis (29,30).

In this study, DJB markedly improved glucose tolerance in obese insulin-resistant rats, and this was accompanied by a striking reduction in insulinemia. Hepatic, skeletal muscle, and adipose tissue insulin sensitivity were substantially improved in DJB animals compared with weight-matched, sham-operated controls. While improved glucose metabolism after bariatric surgery has been widely reported (31–34), improved insulin sensitivity has not always been observed (8,35). For example, while duodenal bypass was shown to improve glucose tolerance, it was not effective at improving insulin sensitivity in high-fat–fed Long-Evans and Wistar rats (8,35). While the underlying reasons for this discrepancy are not clear, it is likely owing to the animal model studied, as discussed above. Since weight gain, food intake, and increasing adiposity proceeded normally in DJB, we conclude that the effects of proximal intestine bypass surgery are due to a mechanism or mechanisms independent of body weight and food intake. Our results from total vagal ligation demonstrate that the rapid restoration of hepatic gluconeogenic capacity and basal HGP in ZF rats is largely regulated by vagal pathways. This finding agrees with recent reports highlighting the key role of upper-intestinal vagal nerves in the regulation of basal HGP (28,36). Importantly, however, the insulin sensitization

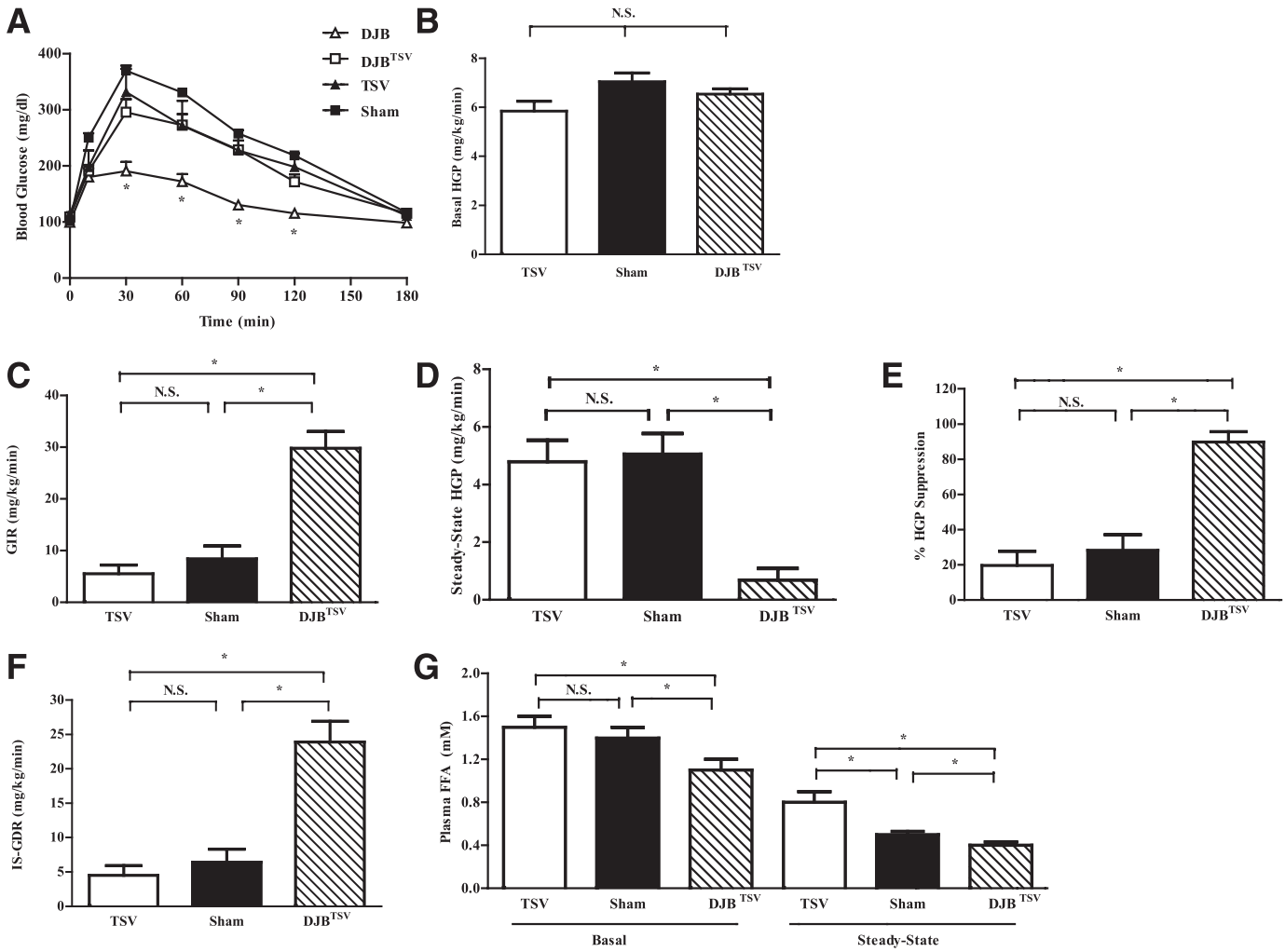

FIG. 6. Vagal innervation is integral for regulation of hepatic gluconeogenic capacity and basal HGP but not hepatic or peripheral insulin sensitivity. *A*: DJB-induced improvement in gluconeogenic capacity is abolished by TSV as assessed by PTT. *B*: TSV abolished DJB-induced improvement in basal HGP as assessed by hyperinsulinemic-euglycemic clamp. *C*: GIR remained elevated in DJB^{TSV} despite total subdiaphragmatic vagal denervation during hyperinsulinemic-euglycemic clamps. This suggests that insulin-sensitization effect of DJB is not mediated by the vagus nerve. *D*: Insulin-stimulated (steady state) HGP remained markedly improved in DJB^{TSV}, suggesting that hepatic insulin sensitization of DJB is not reliant on vagal innervation. *E*: Percent suppression of HGP by insulin during the hyperinsulinemic-euglycemic clamp studies remained elevated in DJB^{TSV} compared with TSV and sham. *F*: IS-GDR, a measure of skeletal muscle insulin sensitivity, was sustained after TSV, suggesting that skeletal muscle insulin sensitization of DJB is not reliant on vagal pathways. *G*: Basal and insulin-stimulated suppression of lipolysis, a measure of adipose tissue insulin sensitivity, is preserved in DJB, suggesting that DJB-induced insulin sensitization of adipose tissue is not reliant on vagal innervation. All experiments were conducted 1 month post-TSV surgery. All experiments consisted of $n \geq 6$/group. *$P < 0.05$. N.S., not significant. Values are means ± SEM.

effect of DJB was independent of vagal innervation. Since reduced food intake, decreased adiposity, or vagal inputs do not appear to be contributing mechanisms to the restoration of insulin sensitivity, an alternative explanation relates to the gastrointestinal tract.

The gastrointestinal tract contains a variety of secretory cells, including enterocytes and enteroendocrine cells, which are specialized neuroendocrine cells responsible for production of a large number of polypeptide hormones. To date, a handful of enterocyte- and enteroendocrine cell–enriched factors have been implicated in regulation of glucose and lipid homeostasis. However, it is quite plausible that the observed changes in the internal milieu of the intestinal tract after DJB, which include an expansion of the intestinal mass, particularly in the ileum, lead to alterations in secreted factors from resident enterocytes and enteroendocrine cells with antidiabetes effects. In support of this hypothesis, we have demonstrated that DJB increases the concentration of GIP and PYY in the jejunum and ileum but not in circulation. In contrast, tissue concentration of GLP-1 was unaltered in DJB, while the circulating concentration was increased.

Several studies have reported increased luminal and circulating concentration of bile acids after bariatric surgery (37–39). Consistent with these studies, we have equally observed an increase in total bile acids in circulation after DJB (Supplementary Fig. 6). In humans, the postprandial rise in serum bile acids is paralleled by an increase in serum concentration of ileum-derived enterokine, fibroblast growth factor (FGF)-19 (FGF-15 in rodents) (40) and has been associated with improved insulin sensitivity after Roux-en-Y gastric bypass (41). Although serum FGF-15 data are lacking in the current study, owing to lack of detection antibodies, we have observed

that FGF-15 mRNA is upregulated by >150% after DJB (42). Therefore, it is plausible that DJB-induced insulin sensitization is in part due to amplified activation of the bile acid–FGF-15/19 axis. In support of this notion and in agreement with the current data, improved glycemic control after FGF-15/19 has been reported to be independent of the Akt/Foxo1 pathway but reliant on the CREB–peroxisome proliferator–activated receptor γ coactivator-1α pathway (43). Lastly, but equally intriguing, are the observations that in obesity, gut-derived factors such as lipopolysaccharides, or even bacteria themselves, can enter the circulation, exerting systemic proinflammatory effects and profound insulin resistance (44–46). Perhaps reengineering of the gastrointestinal tract through changes in bile acids alters gut microflora, or the "leakiness" of bacterial products into the systemic circulation, in such a way that limits these proinflammatory factors.

The improvement in insulin sensitivity and lipid metabolism, particularly in the liver, suggests the possibility of endocrine gastrointestinal factors with potent hepatic effect. In support of this, we found that the hepatic expression of key lipogenic and gluconeogenic genes were markedly reduced, while those involved in β-oxidation were enhanced. It is likely that the reduction in lipogenesis was caused by the decrease in LXR and SREBP-1c expression and decreased ACC expression/activity, while the increased β-oxidation rates were the result of the enhanced AMPK activity. It is of interest that despite an improvement in all parameters of lipid metabolism, hepatic TAG content did not decline in the DJB. This indicates that hepatic TAG content is not directly connected to enhanced hepatic insulin sensitivity; alternatively, our data suggest that DAGs and ceramides may play a more prominent role in the ZF rat. This finding is consistent with previous reports highlighting the association of DAG accumulation with insulin resistance (47,48).

Another surprising observation was the large increase in IRS-2 expression in the DJB. To this end, SREBP-1c has been shown to inhibit IRS-2 transcription by binding to the serum response element site of its promoter (49). Thus, an observed reduction in SREBP-1c expression in DJB may contribute to the increased IRS-2 transcription and subsequent hepatic insulin sensitivity.

In summary, we have demonstrated that selective proximal intestinal bypass ameliorates systemic insulin resistance in ZF rats independent of changes in body weight. Restoration of euglycemia was independent of augmented insulin secretion but was associated with a dramatic improvement in systemic insulin sensitivity, namely, hepatic insulin sensitivity, key insulin signaling molecules, and enhanced tissue-specific substrate metabolism. Importantly, vagal-mediated CNS inputs were essential for the rapid improvement in gluconeogenic capacity and regulation of basal HGP but were not required for the insulin-sensitization effect of DJB in ZF rats. Collectively, the observed morphological changes coupled with altered patterning of the intestinally derived hormone peptides and a robust improvement in glucose homeostasis after DJB support a gastrointestinal-driven mechanism with a potent antidiabetes effect. This work raises the possibility that gut-derived factor(s) responsible for observed beneficial effects could lead the way to the development of new therapeutic approaches for metabolic disease, bypassing the need for bariatric surgery.

ACKNOWLEDGMENTS

This work was supported in part by grants from the National Institutes of Health (DK-033651, DK-074868, and DK-063491).

J.J., J.O., C.M., M.C., J.-Y.H., Y.C., H.T., and M.S. are current and/or past employees of NGM Biopharmaceuticals, Inc. J.M.O. is a member of the scientific advisory board at NGM Biopharmaceuticals, Inc. No other potential conflicts of interest relevant to this article were reported.

J.J. designed and performed the gastrointestinal peptide extraction and measurement, helped write the manuscript, and reviewed and analyzed all datasets. E.J.B. performed real-time PCR and immunoblotting, contributed to discussion, and reviewed and analyzed all datasets. G.B. performed tissue substrate assays, contributed to discussion, and reviewed and analyzed all datasets. J.O. performed glucose tolerance tests, pyruvate tolerance tests, and serum analysis; assisted with clamp procedures; contributed to discussion; and reviewed and analyzed all datasets. C.M. performed substrate assays, real-time PCR, histology, and immunoblotting; designed and wrote the manuscript; contributed to discussion; and reviewed and analyzed all datasets. M.C. performed glucose tolerance tests, pyruvate tolerance tests, and serum analysis; assisted with clamp procedures; contributed to discussion; and reviewed and analyzed all datasets. J.-Y.H. established and evaluated the peptide extraction method and reviewed and analyzed all datasets. Y.C. contributed to the experimental design of the gastrointestinal peptide measurement and reviewed and analyzed all datasets. H.T. contributed to discussion, reviewed the manuscript, and reviewed and analyzed all datasets. J.M.O. designed and wrote the manuscript and reviewed and analyzed all datasets. M.S. designed and wrote the manuscript; conducted all surgeries, in vivo experiments, and tissue analyses; and reviewed and analyzed all datasets. M.S. is the guarantor of this work and, as such, had full access to all the data in the study and takes responsibility for the integrity of the data and the accuracy of the data analysis.

The authors thank Drs. Alex DePaoli and Daniel Kaplan of NGM Biopharmaceutical, Inc., who assisted with editing the manuscript. They also thank Drs. Michael M. Meguid and Carolina G. Goncalves (State University of New York Upstate Medical University) for Roux-en-Y gastric bypass demonstrations.

REFERENCES

1. Schenk S, Saberi M, Olefsky JM. Insulin sensitivity: modulation by nutrients and inflammation. J Clin Invest 2008;118:2992–3002
2. Colquitt JL, Picot J, Loveman E, Clegg AJ. Surgery for obesity. Cochrane Database Syst Rev 2009 (2):CD003641
3. Rubino F. Bariatric surgery: effects on glucose homeostasis. Curr Opin Clin Nutr Metab Care 2006;9:497–507
4. Pories WJ, Swanson MS, MacDonald KG, et al. Who would have thought it? An operation proves to be the most effective therapy for adult-onset diabetes mellitus. Ann Surg 1995;222:339–350; discussion 350–352
5. Speck M, Cho YM, Asadi A, Rubino F, Kieffer TJ. Duodenal-jejunal bypass protects GK rats from beta-cell loss and aggravation of hyperglycemia and increases enteroendocrine cells coexpressing GIP and GLP-1. Am J Physiol Endocrinol Metab 2011;300:E923–E932
6. Xu Y, Ohinata K, Meguid MM, et al. Gastric bypass model in the obese rat to study metabolic mechanisms of weight loss. J Surg Res 2002;107:56–63
7. Guijarro A, Osei-Hyiaman D, Harvey-White J, et al. Sustained weight loss after Roux-en-Y gastric bypass is characterized by down regulation of endocannabinoids and mitochondrial function. Ann Surg 2008;247:779–790
8. Kindel TL, Martins PJ, Yoder SM, et al. Bypassing the duodenum does not improve insulin resistance associated with diet-induced obesity in rodents. Obesity (Silver Spring) 2011;19:380–387

9. Rubino F, Forgione A, Cummings DE, et al. The mechanism of diabetes control after gastrointestinal bypass surgery reveals a role of the proximal small intestine in the pathophysiology of type 2 diabetes. Ann Surg 2006;244:741–749
10. Milne JC, Lambert PD, Schenk S, et al. Small molecule activators of SIRT1 as therapeutics for the treatment of type 2 diabetes. Nature 2007;450:712–716
11. Qi L, Saberi M, Zmuda E, et al. Adipocyte CREB promotes insulin resistance in obesity. Cell Metab 2009;9:277–286
12. Fujita S, Bohland M, Sanchez-Watts G, Watts AG, Donovan CM. Hypoglycemic detection at the portal vein is mediated by capsaicin-sensitive primary sensory neurons. Am J Physiol Endocrinol Metab 2007;293:E96–E101
13. Saberi M, Woods NB, de Luca C, et al. Hematopoietic cell-specific deletion of toll-like receptor 4 ameliorates hepatic and adipose tissue insulin resistance in high-fat-fed mice. Cell Metab 2009;10:419–429
14. Bandyopadhyay GK, Yu JG, Ofrecio J, Olefsky JM. Increased malonyl-CoA levels in muscle from obese and type 2 diabetic subjects lead to decreased fatty acid oxidation and increased lipogenesis; thiazolidinedione treatment reverses these defects. Diabetes 2006;55:2277–2285
15. Seifter S, Dayton S, et al. The estimation of glycogen with the anthrone reagent. Arch Biochem 1950;25:191–200
16. Yoshizaki T, Schenk S, Imamura T, et al. SIRT1 inhibits inflammatory pathways in macrophages and modulates insulin sensitivity. Am J Physiol Endocrinol Metab 2010;298:E419–E428
17. Magnusson I, Rothman DL, Katz LD, Shulman RG, Shulman GI. Increased rate of gluconeogenesis in type II diabetes mellitus. A ^{13}C nuclear magnetic resonance study. J Clin Invest 1992;90:1323–1327
18. Cline GW, Rothman DL, Magnusson I, Katz LD, Shulman GI. ^{13}C-nuclear magnetic resonance spectroscopy studies of hepatic glucose metabolism in normal subjects and subjects with insulin-dependent diabetes mellitus. J Clin Invest 1994;94:2369–2376
19. Koo SH, Flechner L, Qi L, et al. The CREB coactivator TORC2 is a key regulator of fasting glucose metabolism. Nature 2005;437:1109–1111
20. Kakei M, Yada T, Nakagawa A, Nakabayashi H. Glucagon-like peptide-1 evokes action potentials and increases cytosolic Ca2+ in rat nodose ganglion neurons. Auton Neurosci 2002;102:39–44
21. Nakagawa A, Satake H, Nakabayashi H, et al. Receptor gene expression of glucagon-like peptide-1, but not glucose-dependent insulinotropic polypeptide, in rat nodose ganglion cells. Auton Neurosci 2004;110:36–43
22. Koda S, Date Y, Murakami N, et al. The role of the vagal nerve in peripheral PYY3-36-induced feeding reduction in rats. Endocrinology 2005;146:2369–2375
23. Niijima A. Neural control of blood glucose level. Jpn J Physiol 1986;36:827–841
24. Adams TD, Pendleton RC, Strong MB, et al. Health outcomes of gastric bypass patients compared to nonsurgical, nonintervened severely obese. Obesity (Silver Spring) 2010;18:121–130
25. Romijn JA, Corssmit EP, Havekes LM, Pijl H. Gut-brain axis. Curr Opin Clin Nutr Metab Care 2008;11:518–521
26. Pocai A, Obici S, Schwartz GJ, Rossetti L. A brain-liver circuit regulates glucose homeostasis. Cell Metab 2005;1:53–61
27. Cardin S, Walmsley K, Neal DW, Williams PE, Cherrington AD. Involvement of the vagus nerves in the regulation of basal hepatic glucose production in conscious dogs. Am J Physiol Endocrinol Metab 2002;283:E958–E964
28. Cheung GW, Kokorovic A, Lam CK, Chari M, Lam TK. Intestinal cholecystokinin controls glucose production through a neuronal network. Cell Metab 2009;10:99–109
29. Delzenne NM, Cani PD. Gut microbiota and the pathogenesis of insulin resistance. Curr Diab Rep 2011;11:154–159
30. Haeusler RA, Pratt-Hyatt M, Welch CL, Klaassen CD, Accili D. Impaired generation of 12-hydroxylated bile acids links hepatic insulin signaling with dyslipidemia. Cell Metab 2012;15:65–74
31. Cohen RV, Schiavon CA, Pinheiro JS, Correa JL, Rubino F. Duodenal-jejunal bypass for the treatment of type 2 diabetes in patients with body mass index of 22-34 kg/m2: a report of 2 cases. Surg Obes Relat Dis 2007;3:195–197
32. Meirelles K, Ahmed T, Culnan DM, Lynch CJ, Lang CH, Cooney RN. Mechanisms of glucose homeostasis after Roux-en-Y gastric bypass surgery in the obese, insulin-resistant Zucker rat. Ann Surg 2009;249:277–285
33. Patriti A, Aisa MC, Annetti C, et al. How the hindgut can cure type 2 diabetes. Ileal transposition improves glucose metabolism and beta-cell function in Goto-kakizaki rats through an enhanced Proglucagon gene expression and L-cell number. Surgery 2007;142:74–85
34. Stylopoulos N, Hoppin AG, Kaplan LM. Roux-en-Y gastric bypass enhances energy expenditure and extends lifespan in diet-induced obese rats. Obesity (Silver Spring) 2009;17:1839–1847
35. Gavin TP, Sloan RC 3rd, Lukosius EZ, et al. Duodenal-jejunal bypass surgery does not increase skeletal muscle insulin signal transduction or glucose disposal in Goto-Kakizaki type 2 diabetic rats. Obes Surg 2011;21:231–237
36. Wang PY, Caspi L, Lam CK, et al. Upper intestinal lipids trigger a gut-brain-liver axis to regulate glucose production. Nature 2008;452:1012–1016
37. Patti ME, Houten SM, Bianco AC, et al. Serum bile acids are higher in humans with prior gastric bypass: potential contribution to improved glucose and lipid metabolism. Obesity (Silver Spring) 2009;17:1671–1677
38. Nakatani H, Kasama K, Oshiro T, Watanabe M, Hirose H, Itoh H. Serum bile acid along with plasma incretins and serum high-molecular weight adiponectin levels are increased after bariatric surgery. Metabolism 2009;58:1400–1407
39. Kohli R, Kirby M, Setchell KD, et al. Intestinal adaptation after ileal interposition surgery increases bile acid recycling and protects against obesity-related comorbidities. Am J Physiol Gastrointest Liver Physiol 2010;299:G652–G660
40. Lundåsen T, Gälman C, Angelin B, Rudling M. Circulating intestinal fibroblast growth factor 19 has a pronounced diurnal variation and modulates hepatic bile acid synthesis in man. J Intern Med 2006;260:530–536
41. Jansen PL, van Werven J, Aarts E, et al. Alterations of hormonally active fibroblast growth factors after Roux-en-Y gastric bypass surgery. Dig Dis 2011;29:48–51
42. DePaoli A, Ling L, Kaplan D, et al. Fibroblast growth factor 19 (FGF19) is regulated by gastric bypass and mimics the metabolic benefits after the surgery (Abstract). European Association for the Study of Diabetes, 2012
43. Potthoff MJ, Boney-Montoya J, Choi M, et al. FGF15/19 regulates hepatic glucose metabolism by inhibiting the CREB-PGC-1α pathway. Cell Metab 2011;13:729–738
44. de Kort S, Keszthelyi D, Masclee AA. Leaky gut and diabetes mellitus: what is the link? Obes Rev 2011;12:449–458
45. Burcelin R, Serino M, Chabo C, Blasco-Baque V, Amar J. Gut microbiota and diabetes: from pathogenesis to therapeutic perspective. Acta Diabetol 2011;48:257–273
46. Furet JP, Kong LC, Tap J, et al. Differential adaptation of human gut microbiota to bariatric surgery-induced weight loss: links with metabolic and low-grade inflammation markers. Diabetes 2010;59:3049–3057
47. Jornayvaz FR, Shulman GI. Diacylglycerol activation of protein kinase Cε and hepatic insulin resistance. Cell Metab 2012;15:574–584
48. Jornayvaz FR, Birkenfeld AL, Jurczak MJ, et al. Hepatic insulin resistance in mice with hepatic overexpression of diacylglycerol acyltransferase 2. Proc Natl Acad Sci USA 2011;108:5748–5752
49. Ide T, Shimano H, Yahagi N, et al. SREBPs suppress IRS-2-mediated insulin signalling in the liver. Nat Cell Biol 2004;6:351–357